

Extensive near infrared monitoring of millimeter-wave / gamma-ray bright blazars

Alberto Carramiñana, Luis Carrasco, Alicia Porras, Elsa Recillas
 INAOE, Luis Enrique Erro 1, Tonantzintla, Puebla 72840, México

We established a sample of millimeter-wave and γ -ray bright active galactic nuclei matching the *WMAP* catalog with the EGRET catalog, highest energy photons and the *Fermi* bright source list. We have monitored over 80 of these objects in the near infrared, obtaining over 2000 JHKs data points directly comparable with *Fermi* data. We present examples of correlated near infrared and γ -ray activity of known blazars and recently identified sources.

I. MM-WAVE γ -RAY BRIGHT BLAZARS

CGRO-EGRET established the predominance of flat spectrum radio quasars (FSRQ) as extragalactic sources of high-energy γ -rays [1]. These are believed to be powered by supermassive black holes ejecting large amounts of material along relativistic jets perpendicular to accretion disks and producing high energy particles in these jets. Observations at the highest photon energies shown a predominance of Bl Lac objects over FSRQ at $E \sim 1$ TeV. Although these observations may be biased by the horizon limitation due to pair absorption with extragalactic background light (EBL), the *Fermi* γ -ray Space Telescope, more sensitive and more responsive to GeV photons than EGRET, reported a larger fraction of Bl Lac objects among blazars in its bright source list release (0FGL) [2, 3]. The wider spectral coverage of *Fermi* is allowing detailed studies of the intrinsic properties of various types of active galactic nuclei (AGN), cosmic evolution and their use as EBL tracers [4].

The extrapolation of FSRQ to high radio frequencies makes the coincidence of foreground *WMAP* sources with γ -ray blazars expectable. Furthermore, it is clear than most of the 390 *WMAP* sources are AGNs [5]. These emitters are dominated in the mm-wave band by the same synchrotron component observed at lower frequencies and can be expected to emit photons of very high energy, related to the hardest part of the synchrotron emission. *WMAP* sources have fluxes above 0.1 Jy at frequencies $\gtrsim 40$ GHz, making them suitable positional references for large millimeter telescopes. Known common *WMAP*/EGRET sources, found up to $z \gtrsim 2.3$, are relatively nearby analogs of more distant blazars detectable in principle by *Fermi* up to $z \gtrsim 7$ and by the Large Millimeter Telescope (LMT [6]) at $z \gtrsim 30$, if such an object could have existed at such an early phase of the Universe. The combination of *Fermi* and LMT data promises the availability of a sample of thousands of objects up to the highest redshifts ideally suited to study radio loud AGN evolution and the connection of the EBL with the star formation history of the Universe.

II. MATCHING *WMAP* WITH γ -RAY SOURCES

As a by product of the study of the cosmic microwave background, the *Wilkinson Microwave Anisotropy Probe* (*WMAP*) produced a catalog of 390 bright sources detected at frequencies between 23 and 94 GHz, outside a mask defined by the mm-wave emission from the Galactic plane [5]. These objects constitute a fairly homogeneous sample suitable for comparison with all-sky γ -ray catalogs.

We compared the *WMAP* foreground source catalog [5] with: (1) the Third EGRET (3EG) catalog of high-energy γ -ray sources [1]; (2) the $E > 10$ GeV EGRET photons compiled by [7]; (3) the list of bright sources detected with signal-to-noise (\sqrt{TS}) larger than 10 by the *Fermi* γ -ray Space Telescope in its first three months of operations [2]. The positional uncertainty of *WMAP* equals $4'$, similar to that of *Fermi*, but much better than that of EGRET. Preferring to accept false positives than to reject real coincidences, we used a relaxed matching criterion of 2.5 times the combined positional accuracy, $(\sigma_{wmap}^2 + \sigma_{\gamma}^2)^{1/2}$, where σ_{γ} refers to 3EG ($\sim 1^\circ$), EGRET-VHE (0.5°) or 0FGL ($2 - 10'$). For each comparison we estimated the expected number of random coincidences quantifying the solid angle covered by the γ -ray sources (or events) outside the *WMAP* Galactic mask. For each *WMAP*/ γ pair we blindly listed potential radio, optical and X-ray counterparts from SIMBAD / Vizier. The results are listed in tables II and III.

TABLE I: *WMAP* and EGRET source matches by type. (\dagger = excludes P, G and S types [1]).

Source Type	3EG catalog	<i>WMAP</i> mask	Matches	
			Observed	Expected
A	67	54	40	6.6
a	28	23	17	3.3
U	170	61	11	10.0
Total	265 \dagger	138	68	20

TABLE II: em WMAP sources in the 3EG catalog and 0FGL bright source list – Part I. D denotes the integer part of the distance in standard deviations.

WMAP	3EG / 0FGL	D	Counterpart	WMAP	3EG / 0FGL	D	Counterpart
J0050–0649	0FGL J0051.1–0647	[0]	PKS 0048–071	J0334–4007	0FGL J0334.1–4006	[0]	PKS 0332–403
J0051–0927	0FGL J0050.5–0928	[0]	PKS 0048–097	J0339–0143	3EG J0340–0201	[0]	CTA 026
J0108+0135	3EG J0118+0248	[2]	4C 01.02	J0407–3825	0FGL J0407.6–3829	[0]	PKS 0405–385
J0132–1653	3EG J0130–1758	[1]	QSO B0130–171	J0416–2051	3EG J0412–1853	[1]	(QSO B0413–21)??
J0137+4753	0FGL J0137.1+4751	[0]	QSO B0133+47	J0423–0120	0FGL J0423.1–0112	[0]	QSO B0420–015
					3EG J0422–0102	[0]	
J0204+1513	3EG J0204+1458	[0]	4C +15.05	J0428–3757	0FGL J0428.7–3755	[0]	PKS 0426–380
J0205–1704	0FGL J0204.8–1704	[0]	PKS 0202–17	J0442–0017	3EG J0442–0033	[0]	QSO B0440–004
J0210–5100	0FGL J0210.8–5100	[0]	QSO B0208–5115	J0455–4617	3EG J0458–4635	[0]	0454–463
	3EG J0210–5055	[0]					
J0218+0138	0FGL J0217.8+0146	[1]	PKS 0215+015	J0456–2322	0FGL J0457.1–2325	[0]	QSO B0454–234
					3EG J0456–2338	[0]	
J0220+3558	0FGL J0220.9+3607	[0]	B2 0218+35	J0501–0159	3EG J0500–0159	[0]	4C –02.19
J0223+4303	0FGL J0222.6+4302	[1]	3C 66A	J0506–6108	3EG J0512–6150	[1]	0506–612?
	3EG J0222+4253	[0]					
J0237+2848	0FGL J0238.4+2855	[0]	4C +28.07	J0523–3627	3EG J0530–3626	[2]	QSO J0522–3627
	3EG J0239+2815	[1]					
J0238+1637	0FGL J0238.6+1636	[0]	AO 0235+164	J0538–4405	0FGL J0538.8–4403	[0]	PKS 0537–441
	3EG J0237+1635	[1]	QSO B0235+16		3EG J0540–4402	[0]	
J0319+4131	0FGL J0320.0+4131	[0]	NGC 1275	J0539–2844	3EG J0531–2940	[2]	(QSO J0539–2839)??

A. Matching WMAP with EGRET

The comparison between the *WMAP* and 3EG catalogs produced 69 matches out of the 390 *WMAP* and 138 EGRET sources outside the *WMAP* Galactic mask. The number expected randomly is 20; the probability of having 69 matches among the 390 *WMAP* sources is $P \lesssim 10^{-17}$, indicating that most -but not all- the matches are real.

When accounting for the source type we count 40 matches out of the 54 high confidence blazar association, labelled A in the 3EG catalog, compared to 6.6 expected randomly. The low confidence "a" associations have 17 matches out of 23 tries and 3.3 expected chance coincidences. On the other hand we have 11 matches among the 61 unidentified sources out of the *WMAP* mask, expecting 10.0 by chance. On statistical grounds, we can confirm the physical association of foreground *WMAP* sources with 3EG blazars, accounted by both "A" and "a" classes, but not with unidentified EGRET sources (table I).

We also compared the *WMAP* positions with the list of very high energy (VHE) photons, $E > 10$ GeV [7]: 510 out of the 1506 VHE photons are outside the *WMAP* Galactic mask. The combined positional accuracy of VHE photons and *WMAP* sources is 30.2'. We obtained coincidences between 33 VHE photons and 29 *WMAP* sources as follows:

- 20 *WMAP* sources coincide with a single isolated VHE photon;
 - 4 *WMAP* sources coincide with a single VHE photon and a 3EG, with no 0FGL counterpart;
 - 1 *WMAP* source (*WMAP* J1408–0749) coincides with a 3EG source (3EG J1409–0745) and 4 VHE photons (VHE 494, 498, 1058 and 1061) – but with no 0FGL counterpart;
 - 3 *WMAP* sources coincide with VHE photons, 3EG and 0FGL sources; of these *WMAP* J0210–5100 has two VHE photons;
 - 1 *WMAP* source (*WMAP* J0137+4753) coincides with a VHE photon and a 0FGL source (0FGL 0137.1+4751), with no 3EG counterpart.
- We note that given the number and error box sizes of the VHE photons, we expect 30 random matches under our 2.5σ criterion. Most or all of the single *WMAP*-VHE coincidences are likely to be spurious. We note the case of *WMAP* J0137+4753, which belonged to the *WMAP*& VHE only category prior to the publication of the 0FGL and turned out to be a real γ -ray source.

B. Matching the *WMAP* catalog with the *Fermi* bright source list

The *Fermi* bright source list (0FGL), made public in February 2009, consists of 205 bright γ -ray sources detected with significance $\sqrt{TS} > 10$ in the first three months of observations [2]. Of these, 121 are of the AGN class, mostly blazars [3]. The 0FGL list has 122 objects outside the *WMAP* Galactic mask, which we compared with the respective *WMAP* and *Fermi* positions. The improved positional accuracy of *Fermi*, in the $4' - 10'$ range, results in only 0.82 spurious coincidences expected. We found 54 matches between *WMAP* and the 0FGL, 25 of which are common with EGRET sources and 29 are independent.

C. Sample overview

The sample is presented in tables II and III. The *D* column expresses the distance between the *WMAP* and the γ -ray event in terms of the integer part of the combined positional accuracy; associations with [0] have intersecting error contours and are more likely to be real than those with [2], separated by $\geq 2\sigma$. Most of the sources have a suitable radio, optical and/or X-ray counterpart, often in the intersection of the *WMAP*/ γ -ray error boxes. In a few cases the candidate counterpart is not unique and the one displayed is a subjective election. Counterparts in parenthesis are tentative. We note the following:

- *WMAP* J0051–0927 :: 0FGL J0050.5–0928 has a preferred association with the Bl Lac object PKS 0048–071 = PHL 856; the radiogalaxy FIRST J005051.9–092529 is an alternative.
- *WMAP* J0237+2848 :: 0FGL J0238.4+2855 :: 3EG J0239+2815. This is listed as a low confidence *Fermi* association with 4C +28.07 in [2]. The *WMAP* and *Fermi* boxes match, both containing 4C +28.07. All are somewhat outside the EGRET box.
- *WMAP* J0319+4131 :: 0FGL J0320.0+4131 is identified with the radiogalaxy NGC 1275. We note that the radiogalaxy Cen A is excluded of this study by the *WMAP* Galactic mask.
- *WMAP* J0423–0120 :: 0FGL J0423.1–0112 :: 3EG J0422–0102. This is a low confidence *Fermi* association with PKS 0420–014, which is at the center of the *WMAP* circle.
- *WMAP* J0909+0119 :: 0FGL J0909.7+0145. The 0FGL error radius is $17'$, the *WMAP* and 0FGL positions differing by $25'$. PKS 0907+022 is a low confidence *Fermi* association not compatible with *WMAP*. 4C+01.24 (PKS =

QSO B0906+015) is inside the *WMAP* box and marginally compatible with the *Fermi* source.

- *WMAP* J1517–2421 has two possible EGRET counterparts but only one (3EG J1517–2538) is compatible with the 0FGL source.
- *WMAP* J1642+3948 is $19'$ away from 0FGL J1641.4+3939, which has an positional error of $9.5'$, making the association tentative. There are suitable candidates for both sources, with 3C345 being positionally the best *common* counterpart, as discussed in §VC. While there is no 3EG source association, we note the revised EGRET counterpart EGR J1642+3940 [8].

III. NEAR INFRARED MONITORING

On August 2007, we started a dedicated monitoring program with up to 60 nights per semester awarded on the 2.1m telescope of the Observatorio Astrofísico Guillermo Haro (OAGH), in Cananea, Sonora, Mexico (lat=+31.05, long=–110.38). The program consists of optical photometry (BRVI), low resolution spectroscopy (4000 - 7500 Å) and near infrared JHKs imaging of the sample above, with the addition of high priority *GLAST/Fermi* sources and targets notified via the multi-wavelength *Fermi* group. The current study is to lead to programs of follow-up and identification of γ -ray sources using near infrared, optical and mm-wave facilities.

Particularly successful has been the JHKs photometric survey using the CANanea Near Infrared CAmera (CANICA). CANICA is equipped with a Rockwell 1024×1024 pixel Hawaii infrared detector working at 75.4 K with standard near infrared filters. The scale plate is $0.32''/\text{pixel}$. Observations are usually carried out in series of dithered frames in each filter. Datasets are coadded after correcting for bias and flat-fielding using IRAF based macros. Figure 1 shows the photometric magnitudes measured with CANICA, with detection thresholds around magnitudes 19, 18 and 17 for J, H and Ks respectively, i.e. about two magnitudes fainter than 2MASS.

IV. CORRELATED INFRARED/ γ -RAY ACTIVITY

We have found correlated infrared and γ -ray correlations with little or no evidence for time delays in our sample. We show here joint CANICA H band ($1.6\mu\text{m} \Rightarrow 0.76\text{eV}$) and *Fermi* (1 – 300 GeV) light curves, normalizing the maximum γ -ray flux to the maximum H-band flux and setting both zeros at the same level. We are currently studying the infrared

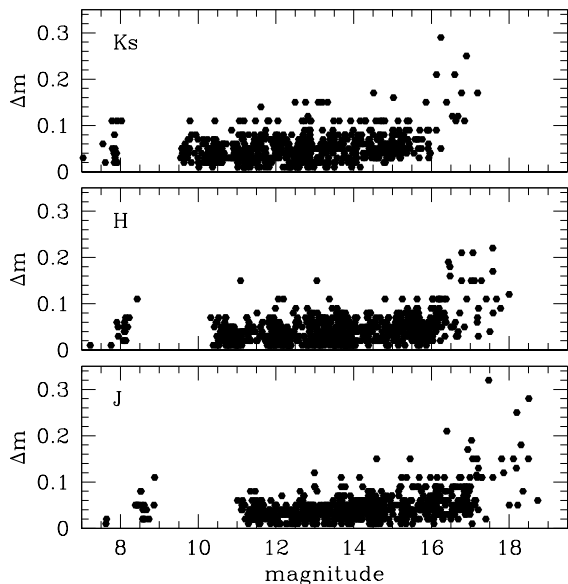


FIG. 1: CANICA photometric measurements of mm-wave/ γ -ray sources. We show only detections.

color behavior of our sample during flares and constraining possible delays in the timing of near infrared flares relative to the γ -ray ones. Our current results on 3C 454.3 are presented in [9].

A. PKS 0235+164

PKS 0235+164 is positionally coincident with WMAP J0238+1637, mm-wave source coincident with 3EG J0237+1635 = 0FGL J0238.6+1636. The WMAP source is labelled as probable variable. Figure 2 shows the joint H band and 1-300 GeV fluxes scaled. The near infrared flux at the end of 2008 and beginning of 2009 matched the 2MASS values. On JD2454715 we found PKS 0235+164 almost three magnitudes brighter, prior to peaking 25 days later in coincidence with the *Fermi* flare.

B. PKS 0454-234

The WMAP and *Fermi* error circles in this region of the sky intersect close to the center of the 3EG J0456-2338 error box. PKS 0454-234 is within the intersection, in a neat positional match. We started monitoring on JD 2454748, when the near infrared flux was 0.85 magnitudes above the 2MASS reference value. The source flared by a factor of nearly 3 in the next 50 days to drop to a half 18 days later. The near infrared peak seems delayed by about a week relative to the 1-300 GeV maximum. The AGN has been in

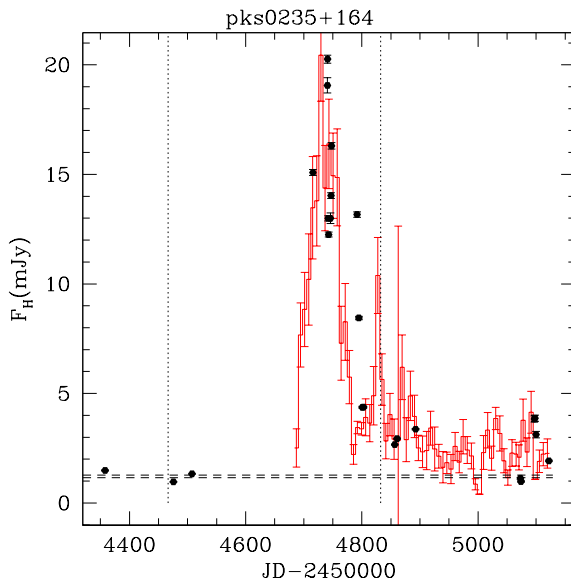


FIG. 2: Joint CANICA - *Fermi* light curve of PKS 0235+164. CANICA is given by the (black) points while *Fermi* fluxes form the (red) histogram with error bars. The discontinuous horizontal line marks the 2MASS flux. The dotted vertical lines indicate the change of year.

relative quiescence since (fig. 3).

C. PKS 1510-089

PKS 1510-89 is the high confidence counterpart of 3EG J1512-0849, WMAP J1512-0904 and 0FGL J1512.7-0905, with an excellent positional match between all data. We started monitoring PKS 1510-89 in early 2008, a few months prior to the *Fermi* launch, when the flux fluctuated around the 2MASS reference value. We caught a simultaneous infrared - γ -ray flare on JD 2454924 and the subsequent decay a month later.

V. SOURCE IDENTIFICATIONS

A. The identification of QSO B0133+476

QSO B0133+476 is a rather active quasar first catalogued originally as DA55 in the Dominion DA 1420 MHz survey [10]. Also known as Mis V1436, archival optical data exists since at least 1953, when it was around magnitude $R=18.7$. This object has been monitored by other groups since 2007, when it was found to be 4.5 magnitudes brighter. Its optical variability is well documented in [11].

This object has no EGRET counterpart, the only evidence for γ -ray emission prior to the *Fermi* launch

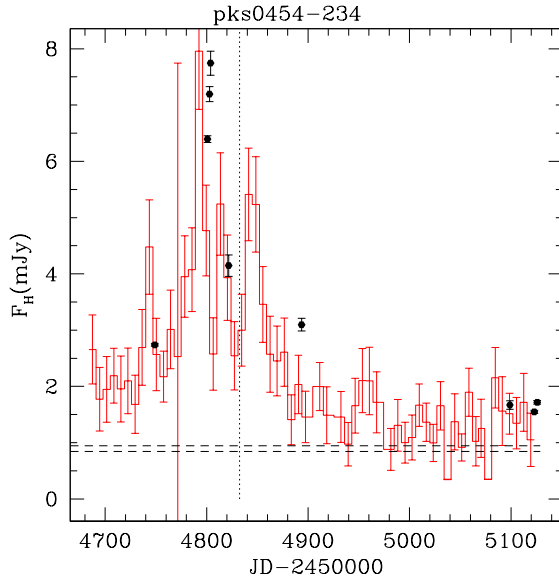


FIG. 3: Joint CANICA - *Fermi* light curve of PKS 0454-234. The discontinuous horizontal line marks the 2MASS flux. The dotted vertical lines indicate the change of year.

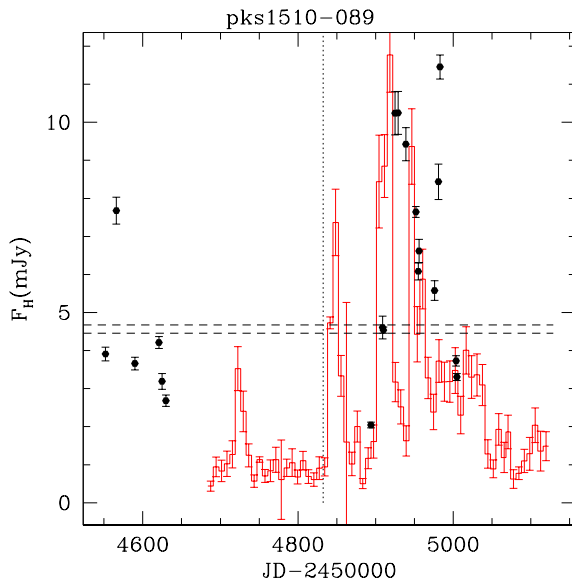


FIG. 4: CANICA - *Fermi* light curve of PKS 1510-089. The discontinuous horizontal line marks the 2MASS flux. The dotted vertical lines indicate the change of year.

being its marginal closeness to a $85(\pm 38)$ GeV photon. The unprovable association of this single photon with QSO B0133+476 is of interest as its energy is close to the pair absorption EBL limit for the redshift of the object, $z = 0.859$. If true, this association would indicate the potential of this source for testing the EBL horizon using *Fermi*, specially under phases of high

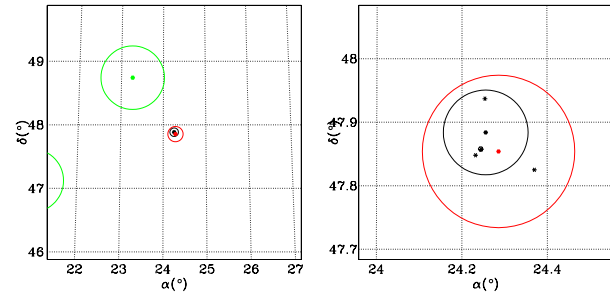


FIG. 5: Positional circumstance of QSO B0133+476. *Left*: the VHE photon error circle is shown at $\alpha \sim 23^\circ$, $\delta \sim 48.6^\circ$, with the almost concentric *WMAP* and *Fermi* circles in the middle. *Right*: a zoom panel showing the $4'$ *WMAP* circle contained in the $7'$ *Fermi* position. QSO B0133+476 is indicated by the open hexagon and an asterisk.

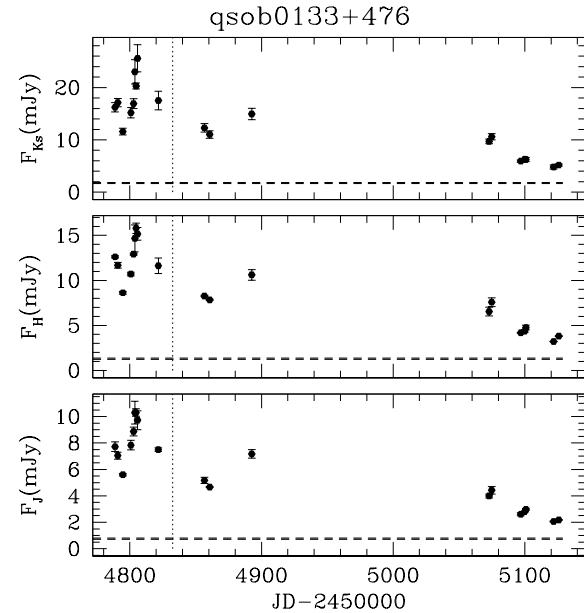


FIG. 6: CANICA light curve of QSO B0133+47. The flaring at the end of 2008 is clearly visible, at a factor of 10 above the 2MASS flux levels indicated by the dashed horizontal line.

emission activity. Our report of near infrared flaring from data taken between JD 2454788 and 2454795 [12] was followed by the *Fermi* detection report, at a flux level above the EGRET limiting sensitivity [13]. The infrared light curve is shown in figure 6. The object was caught undergoing a rapid flare which has declined relatively slowly during 2009, but always at levels above 2MASS.

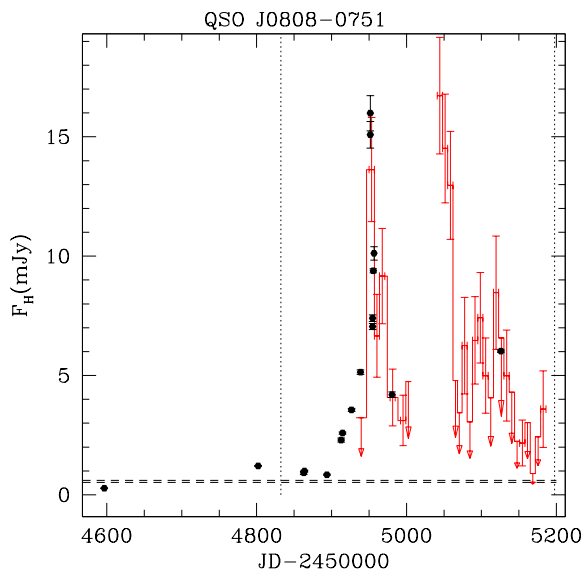


FIG. 7: CANICA - *Fermi* QSO J0808-0751 light curve. The dots indicate the H band fluxes in mJy, while the histogram and upper limit arrows indicate the 1-300 GeV fluxes and limits in scaled units. The discontinuous horizontal line marks the 2MASS flux. The dotted vertical lines indicate the change of year.

B. QSO J0808-0751

The EGRET source 3EG J0812-0646 was not in the high priority *GLAST/Fermi* list, with the association with QSO J0808-0751 been only tentative ($D = 2$). WMAP J0808-0750 is somewhat displaced from the 3EG location, but contains this $z = 1.84$ QSO. The rapid flare observed simultaneously in the near infrared and by *Fermi* of this source, not in the 0FGL, confirms the identity of the QSO as the γ -ray source. We missed a second flare occurring while the source was on the daylight. The flux increase in the near infrared reached a factor of ten within 50 days.

C. The identification of 0FGL J1641.4+3939 with 3C 345

The angular distance between WMAP J1642+3948 and 0FGL J1641.4+3939 is $19.2' = 1.9\sigma$ times the combined positional uncertainty, the association between both objects being tentative only. This is a rather populated region of the sky, where several potential counterparts can be found for each object: - candidate counterparts of 0FGL J1641.4+3939 include 3C 345, QSO B1641.5+3956, QSO

B1641.6+3949, QSO B1640+398, QSO
B1641.8+3956, QSO B1641+3958, QSO
B1640.5+3944, QSO B1640+396, three more QSOs,

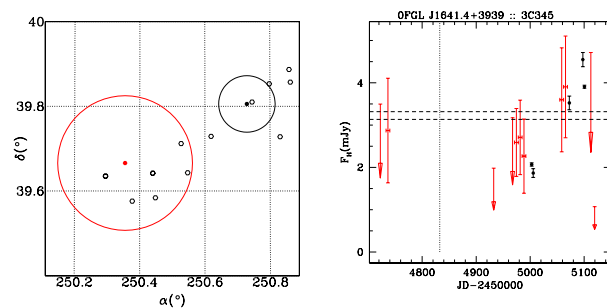


FIG. 8: *Left*: position of 0FGL J1641.4+3939 (larger circle) and WMAP J1642+3948 (smaller circle) with a few potential counterparts (AGN class - open hexagons). *Right*: CANICA H band light curve of 3C345 compared with the (1-300 GeV) fluxes from 0FGL J1641.4+3939 by *Fermi*. The discontinuous horizontal lines mark the 2MASS flux and error. The dotted vertical line indicates the change of year.

a Seyfert 1 and a radiogalaxy from SDSS. - potential counterparts for WMAP J1642+3948 are GB6 J1642+3948 = 3C 345, FIRST J164304.3+394836, QSO B1641+3949, ... 3C 345 has a lower χ^2 relative to the combined *WMAP* and *Fermi* positions (fig. 8), being the best candidate under the assumption of a common association. Even though more data are desirable, the simultaneous flux changes measured provide evidence for the physical association between 0FGL 1641.4+3939 and 3C345.

VI. SUMMARY

We have selected a sample of mm-wave/ γ -ray bright blazars from the *WMAP*, 3EG catalogs and 0FGL list. We have monitored these in the near infrared finding correlated variability, which has also allowed the identification or confirmation of some of these objects.

Acknowledgments

We acknowledge the use of 2MASS, WMAP, Fermi, SIMBAD, VizieR and POSS databases. We appreciate the support of the technical staff at the Observatorio Astrofísico Guillermo Haro.

-
- [1] Hartman, R.C., et al. 1999, ApJS 123, 79.
 - [2] Abdo, A.A., et al. 2009a, ApJS 183, 46.
 - [3] Abdo, A.A., et al. 2009b, ApJ 700, 597.
 - [4] Dermer, C.D. 2007, AIP Conf. Proc. 921, 122.
 - [5] Wright, E.L., et al. 2009, ApJS 180, 283.
 - [6] Serrano Pérez-Grovas, A., Schloerb, F.P., Hughes, D., Yun, M. 2006, SPIE 6267, 1.
 - [7] Thompson, D.J., Bertsch, D.L., O'Neal Jr., R.H. 2005, ApJS 157, 324.
 - [8] Casandjian, JM, Grenier, IA. 2008, A&A 489, 849.
 - [9] Carramiñana, A., Carrasco, L., Chavushyan, V. et al. 2009, Fermi Symposium eConf proceedings.
 - [10] Galt, J.A., Kennedy, J.E.D. 1968, AJ 73, 135.
 - [11] <http://www.aerith.net/misao/variable/MisV1436.html>
 - [12] Carramiñana, A., Carrasco, L., Recillas, E., Chavushyan, V. 2008, ATEL 1874.
 - [13] Takahashi, H., Tosti, G. on behalf of the Fermi-LAT collaboration 2008, ATEL 1877.

TABLE III: WMAP sources in the 3EG catalog and 0FGL bright source list.

WMAP	3EG / 0FGL	D	Counterpart	WMAP	3EG / 0FGL	D	Counterpart
J0720-6222	3EG J0702-6212	[2]	...	J1510-0546	0FGL J1511.2-0536	[0]	PKS 1508-05
J0721+7122	0FGL J0722.0+7120 3EG J0721+7120	[0] [0]	PKS 0716+714	J1512-0904	0FGL J1512.7-0905 3EG J1512-0849	[0] [0]	QSO B1510-089
J0738+1743	0FGL J0738.2+1738 3EG J0737+1721	[0] [0]	QSO B0735+178	J1517-2421	0FGL J1517.9-2423 3EG J1517-2538 ^a	[0] [1]	QSO B1514-241
J0808-0750	3EG J0812-0646	[2]	QSO J0808-0751	J1608+1027	3EG J1608+1055	[0]	4C +10.45
J0813+4817	3EG J0808+4844	[1]	(4C+48.22)	J1613+3412	3EG J1614+3424	[1]	QSO B1611+343
J0825+0311	3EG J0828+0508	[2]	QSO B0823+033	J1642+3948	0FGL J1641.4+3939	[1]	(4C+39.48)?
J0831+2411	3EG J0829+2413	[0]	QSO J0830+2411	J1654+3939	0FGL J1653.9+3946	[1]	Mrk 501
J0841+7053	3EG J0845+7049	[0]	0836+710	J1703-6214	3EG J1659-6251	[1]	
J0854+2006	0FGL J0855.4+2009 3EG J0853+1941	[0] [0]	OJ 287	J1736-7934	3EG J1720-7820	[2]	PKS 1725-795
J0909+0119	0FGL J0909.7+0145	[1]	PKS 0907+022	J1740+5212	3EG J1738+5203	[0]	QSO B1739+522
J0920+4441	0FGL J0921.2+4437 3EG J0917+4427	[0] [1]	RGB J0920+446	J1800+7827	0FGL J1802.2+7827	[0]	S5 1803+78
J0957+5527	0FGL J0957.6+5522 3EG J0952+5501	[0] [1]	4C +55.17	J1820-6343	3EG J1813-6419	[1]	
J0959+6530	3EG J0958+6533	[0]	QSO B0954+65	J1848+3223	0FGL J1847.8+3223	[0]	TXS 1846+322?
J1058+0134	0FGL J1057.8+0138	[0]	PKS 1055+018	J1849+6705	0FGL J1849.4+6706	[0]	S4 1849+67
J1059-8003	0FGL J1100.2-8000	[0]	PKS 1057-79	J1923-2105	0FGL J1923.3-2101 3EG J1921-2015	[0] [1]	PMN J1923-2104
J1130-1451	0FGL J1129.8-1443	[0]	PKS 1127-14	J1937-3957	3EG J1935-4022	[2]	
J1147-3811	0FGL J1146.7-3808 3EG J1134-1530	[0] [2]	PKS 1144-379	J1939-1525	3EG J1937-1529	[0]	QSO B1939-155
J1159+2915	0FGL J1159.2+2912 3EG J1200+2847	[0] [0]	4C +29.45	J2011-1547	3EG J2020-1545	[2]	QSO B2008-159
J1223-8306	3EG J1249-8330	[1]		J2035+1055	3EG J2036+1132	[1]	QSO B2032+107
J1229+0203	0FGL J1229.1+0202 3EG J1229+0210	[0] [0]	3C 273	J2056-4716	0FGL J2056.1-4715 3EG J2055-4716	[0] [0]	PMN J2056-4714
J1246-2547	0FGL J1246.6-2544	[0]	PKS 1244-255	J2143+1741	0FGL J2143.2+1741	[0]	OX 169
J1256-0547	0FGL J1256.1-0547 3EG J1255-0549	[0] [1]	3C 279	J2151-3027	3EG J2158-3023	[2]	PKS 2155-304
J1310+3222	0FGL J1310.6+3220	[0]	B2 1308+32	J2202+4217	0FGL J2202.4+4217 3EG J2202+4217	[0] [0]	Bl Lac
J1316-3337	3EG J1314-3431	[1]	QSO B1313-333	J2203+1723	0FGL J2203.2+1731	[0]	PKS 2201+171
J1327+2213	(3EG J1323+2200)?	[2]	QSO B1324+224	J2207-5348	0FGL J2207.0-5347	[0]	PKS 2204-54
J1337-1257	3EG J1339-1419	[1]	QSO B1335-127	J2211+2352	3EG J2209+2401	[0]	QSO B2209+236
J1354-1041	0FGL J1355.0-1044	[0]	PKS 1352-104	J2229-0833	0FGL J2229.8-0829	[0]	QSO B2227-088
J1408-0749	3EG J1409-0745	[0]	QSO B1406-074	J2232+1144	0FGL J2232.4+1141 3EG J2232+1147	[0] [0]	CTA 102
J1419+3822	3EG J1424+3734	[1]	QSO B1417+385	J2254+1608	0FGL J2254.0+1609 3EG J2254+1601	[0] [0]	3C 454.3
J1427-4206	3EG J1429-4217	[0]	QSO B1424-418	J2322+4448	3EG J2314+4426	[2]	GB6 B2319+4429
J1457-3536	0FGL J1457.6-3538 3EG J1500-3509	[0] [0]	PKS 1454-354	J2327+0937	0FGL J2327.3+0947	[0]	GB6 B2325+0923
J1504+1030	0FGL J1504.4+1030	[0]	PKS 1502+106	J2349+3846	3EG J2352+3752	[1]	QSO B2346+385
J1506-1644	3EG J1504-1537	[1]	(QSO B1504-1626)	J2354+4550	3EG J2358+4604	[1]	4C 45.51